

2D pattern evolution constrained by complex network dynamics

L. E. C. da Rocha and L. da F. Costa*

*Grupo de Pesquisa em Visão Cibernética, Instituto de Física de São Carlos,
Universidade de São Paulo, Av. Trabalhador São Carlense 400,
Caixa Postal 369, 13560-970, São Carlos, SP, Brazil*

(Dated: 29th September 2006)

Abstract

Complex networks have established themselves along the last years as being particularly suitable and flexible for representing and modeling several complex natural and human-made systems. At the same time in which the structural intricacies of such networks are being revealed and understood, efforts have also been directed at investigating how such connectivity properties define and constrain the dynamics of systems unfolding on such structures. However, lesser attention has been focused on hybrid systems, *i.e.* involving more than one type of network and/or dynamics. Because several real systems present such an organization (*e.g.* the dynamics of a disease coexisting with the dynamics of the immune system), it becomes important to address such hybrid systems. The current paper investigates a specific system involving a diffusive (linear and non-linear) dynamics taking place in a regular network while interacting with a complex network of defensive agents following Erdős-Rényi and Barabási-Albert graph models, whose nodes can be displaced spatially. More specifically, the complex network is expected to control, and if possible to extinguish, the diffusion of some given unwanted process (*e.g.* fire, oil spilling, pest dissemination, and virus or bacteria reproduction during an infection). Two types of pattern evolution are considered: Fick and Gray-Scott. The nodes of the defensive network then interact with the diffusing patterns and communicate between themselves in order to control the spreading. The main findings include the identification of higher efficiency for the Barabási-Albert control networks.

PACS numbers: 89.75.Hc,89.75.Kd,05.45.-a,02.70.Rr

*Electronic address: luciano@if.sc.usp.br

I. INTRODUCTION

Complex systems have always motivated intense scientific research. In the last decades, much attention has been focused on systems involving strongly interacting agents. More recently, tools provided by the theory of complex networks have been successfully applied in order to characterize the structure of many of such systems [1, 2, 3]. Once the system of interest is properly translated into a network, its structural properties [1, 3, 4, 5] can be calculated and used to characterize and analyze the system as well as dynamical processes being underlined by the network [1, 6, 7, 8, 9]. However, many dynamics are often related to processes taking place outside the network, possibly also over some network (the same or different). Such systems have received scant attention from the complex network community.

The current paper investigates the evolution of dynamical systems underlined by two distinct (but coexisting) networks, which are henceforth called *disease* and *antidote*. Note that this specific terminology is adopted here only for the sake of simplicity; the proposed model and dynamics are valid for many situations (*e.g.* fire spread, oil spilling, pest control, etc.) other than diseases and inflammatory processes. The first system, involving a complex network of the Erdős-Rényi – ER [10] or Barabási-Albert – BA [11] type, senses and interact with the other system, here represented by a *regular network* over which linear (Fick [12]) and non-linear (Gray-Scott [13]) pattern formation is allowed to evolve. The Fick diffusion model provides a linear, homogeneous and isotropic flux of mass from a fixed and infinite source. The Gray-Scott reaction-diffusion dynamics produces non-static, growing patterns without well-defined sources. Examples of such situations include forest fires, where the nodes of the complex networks represent firemen, organized into communicating groups, trying to stop the spreading of the fire, represented by a diffusive process in the regular network. Other similar situations include oil spilling (oil diffusing along the regular network, while a complex network of cleaners try to control the process) and the evolution of a disease along a healthy tissue, with the nodes representing the defensive cells trying to self-organize in order to control and stop the disease. Observe that the connections established by the agents of the system are not necessarily physical. In fact, these connections may correspond to wireless communication, bio-chemical signaling or even intermediate agents (as modeled in *bi-partite graphs*), *e.g.* enzymes in biological networks.

The article starts by presenting the pattern formation models (Fick and Gray-Scott) and proceeds by describing the interaction between the two involved networks (*i.e.* *regular* and *complex*).

The results and discussion follow, and the article is conclude by emphasizing the main contributions and perspectives for future developments.

II. DIFFUSION MODELS

Over the twentieth century, a number of natural phenomena have been modeled by diffusion and pattern formation processes. The former type of dynamics includes the established topics of atoms and molecules diffusion [14] as well as heat diffusion through different materials [15]. In addition, econometricians have developed diffusion models to forecast the acceptance of new products and the understanding of their life-cycle [16]. Migration of animals and spreading of organisms and chemical substances are often investigated in terms of biological diffusion models [17]. More recently, complex biological and chemical patterns have been reproduced by systems of equations with diffusive and reactive terms [18]. These models range from simple diffusion equations (*e.g.* heat diffusion in a rod) to more sophisticated advection-diffusion (*e.g.*, chemical oceanography) and reaction-diffusion equations (*e.g.*, chemical and biological patterns). Two of such models are considered in the present paper in order to represent a reasonably representative range of natural and artificial phenomena: Fick diffusion and the Gray-Scott reaction-diffusion models.

The Fick diffusion model of an entity U is represented in eq. (1). It can be derived from the continuity equation [12]. The concentration u of U evolve in time proportionally to the difference between the average value of u around a given point and the value of u at that point. The proportionality constant is given by the diffusion coefficient D_u .

$$\frac{\partial u}{\partial t} = D_u \nabla^2 u \quad (1)$$

The Gray-Scott model includes the following two irreversible reactions [13]:



where U and V are two reacting specimens and P an inert precipitate. Considering the concentrations of specimens U and V , respectively as u and v , these reactions can be expressed by a pair of non-linear partial differential equations (3) with diffusive and reactive terms.

$$\frac{\partial u}{\partial t} = D_u \nabla^2 u - uv^2 + f(1 - u) \quad (3)$$

$$\frac{\partial v}{\partial t} = D_v \nabla^2 v + uv^2 - (f + k)v$$

where D_u and D_v are the diffusion coefficients. The dimensionless feed rate of the first reaction is f ; k is the dimensionless rate constant of the second reaction.

III. DIFFUSION AND DEFENSE DYNAMICS

Both diffusion models were evaluated on a spatial mesh (*i.e.*, a regular network) of 256 by 256 points with periodic boundary conditions. The system size was 3.0 in both directions. Numerical integrations were carried out by the forward Euler method of the finite-difference equations resulted from discretization of the diffusion operator. The time step was 1 time unit. The diffusion coefficients were set as $D_u = 0.00002$ (to both diffusion models) and $D_v = 0.00001$. A complex network was used to represent the agents (*i.e.*, nodes) susceptible to be activated by the regular network. There were two states associated to each node: *susceptible* or *activated*. All the nodes began in the susceptible state. As soon as the disease overcame a threshold at the node spatial position (x, y) , or in case the node is requested to help its neighbors, the node was turned to the activated state. In case a node is requested simultaneously as a consequence of high activity in the regular network and by one of its neighbors in the complex network, priority is given to the former situation. After a while, the node returned to the susceptible state.

Two configurations of initial conditions were investigated. In the first configuration (fig. 1-a), the entire system was placed in the uninfected state: $U(x, y) = 0$ (Fick model) and, $U(x, y) = 1$ and $V(x, y) = 0$ (Gray-Scott model). The source of the disease, a 11 by 11 square mesh points, was centered in the middle of the board and set as $U(x, y) = 1$ (Fick model), and $U(x, y) = 0.5$ and $V(x, y) = 0.25$ (Gray-Scott model). In the latter model, the source was perturbed by adding random values of ± 0.01 , in order to break the square symmetry. The node were randomly distributed inside a rectangular area (one third of the board area, with 256 by 85 points) on the left side of the mesh, at 38 mesh points away from the disease source. Initially, all the node were set to the susceptible state. This simple arrangement was chosen to create a "wall" of node and contributed to the vertical symmetry of the configuration, reducing the number of parameters to be considered during simulation.

In the second configuration (fig. 1-b), the node were distributed inside the same rectangular region as before, but the area was centered in the middle of the mesh. The source was broken

in two (11 by 6 rectangular mesh points each piece), to correspond to about the same amount of initial disease. Both sources were symmetrically placed at same distance (*i.e.*, 38 mesh points) and opposite sides from the nodes "wall". This assembly induced a competition for neighbors of activated node.

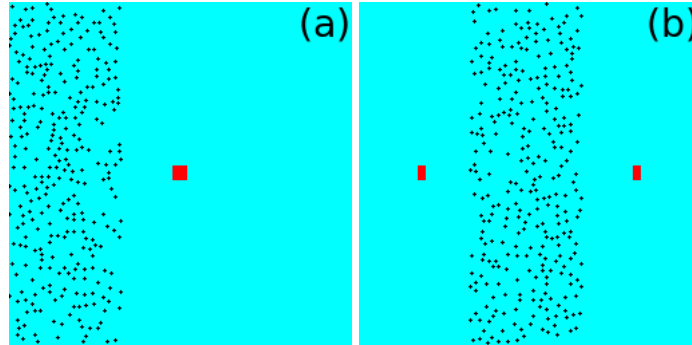


Figure 1: Two configurations of initial conditions for the Fick diffusion model: (a) one source and (b) two sources. Similar initial conditions were used for the Gray-Scott model, except for the source value.

In the Fick model, a node became activated when the disease overcame a threshold $T_U(x, y) = 0.4$ at the respective node position, *i.e.*, x and y . In the Gray-Scott model, the disease must fall below a threshold $T_U(x, y) = 0.6$ in order to activate the node. Remember that absence of disease was represented by $U(x, y) = 0$ in the Fick model and by $U(x, y) = 1$ in the Gray-Scott model. As soon as a node had been activated, all its topological neighbors were requested to help (see fig. 2). The engaged neighbors were randomly distributed at distance $R = 5$ from the activated node. In order to avoid overlapping in the liberation of antidote, a circular area of influence (with radius $R_i = 5$) was defined around every node, so that no other activated node was included within this area. In fact, we guaranteed a minimum distance ($R = R_i = 5$) between any two activated node, ensuring a compact distribution of the node. Once this circle was filled, the remaining nodes were assembled at double the initial radius, and so on (see, for example, the node with a *star* in fig. 2). The antidote liberation consisted in keeping for 50 time units an opposite Fick diffusion from all activated nodes with $D_a = 0.00003$, and intensity $I_a(x, y) = 1$ (Fick model) and $I_a(x, y) = 10$ (Gray-Scott model). The higher intensity is necessary in the latter model because of the fast moving characteristic of this reaction-diffusion. Observe that the activated time is calculated so as to liberate enough antidote within the circular area of influence of the node, reducing the overlap between different nodes. Afterwards, the node ceased its activity and returned to the susceptible

state. If two node requested help from the same neighbor, the latter chose one of them with equal probability.

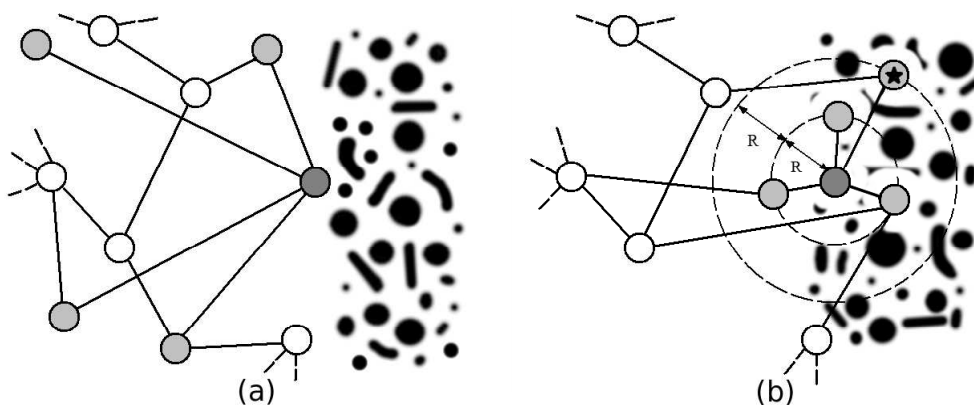


Figure 2: Diagram illustrating a *sub-network* (a) before and (b) after the node activation. The dark-gray node was spatially activated by the disease and the four light-gray node were the topologically activated helpers.

IV. RESULTS

The suggested dynamics involving the interaction between two networks always resulted in competition between the disease and the antidote, where the winner was ultimately a consequence of the values chosen for the diffusion and defense parameters. Some parameter configurations have been observed to lead to a situation where great part of the effort to control the disease was wasted. On the other hand, it was possible to find parameter configurations where the defense always succeed, *i.e.*, the disease vanished. Once such parameters were identified and adopted, we compared the role of the network structure in the proposed defense dynamics.

Figure 3 presents snapshots of the evolution of the disease for four cases assuming the *one-source* configuration. A set of movies with all the configurations discussed in this paper can be viewed at <http://cyvision.ifsc.usp.br/~luisrocha/paper/>. The first two rows show the evolution of the Fick diffusion controlled by (a) ER and (b) BA defensive networks, both with 300 node and $\langle k \rangle \approx 4$. In this case, the activation of the first node only took place after a relatively long period of time. More precisely, the first activation (not shown in the figures) occurred about 8200 time units before the first snapshot in the ER case and about 3600 time units in the BA case, but they

had little effect on disease control. However, these early activations were important because they brought some node closer to the disease source. As soon as some node were close enough to the source, they were activated, triggering a chain activation effect (first snapshot in fig. 3-a). The latter effect occurred because some of the activated node fell at positions where the disease had already overcome the threshold (second snapshot in fig. 3-a). Hence, the spatially activation of the node resulted on requests to their own neighbors, and so on. Observe the *hub* activation in the BA case (first snapshot in fig. 3-b). In this case, many activated node were requested at once and, consequently, some of them fell very near the source. As a result, their own neighbors (*i.e.* the neighbors of the neighbors of the hub) were activated, consequently populating the area around the source and enclosing it with a considerable amount of antidote (second snapshot in fig. 3-b). The ER network node took three times longer to achieve the control of the source (third snapshot in fig. 3-a), *i.e.* to encircle the source. After this stage of the chain reaction, the source became enclosed and the node kept on changing their states. Each new spatial activation redistributed the helpers around the source and even requested node which had never been activated before. The latter effect, *i.e.* the activation of the *hubs*, implied in the fastest decrease in the total quantity of the disease considering the BA network (fourth snapshot in fig. 3-b). At the last considered snapshot, the mesh was found to be more free of disease in the BA case, while a substantially more infected configuration was observed in the ER cases (fifth snapshot in fig. 3-a). After very long times, the in node ended to converge around the source.

The chosen configuration of the Gray-Scott reaction-diffusion ($f = 0.04$ and $k = 0.064$) generated non-static patterns whose spots and stripes tended to quickly reach the complex network. Figures 3-c and 3-d, represent the reaction-diffusion evolution constrained by the ER and BA defensive networks, respectively, with 300 node and $\langle k \rangle \approx 4$ each. After the first node activation (first snapshot in fig. 3-c,d), a chain reaction was triggered as in the Fick diffusion model. The node were activated from the center to the boundary of each case (second snapshot in fig. 3-c,d), a natural consequence of the dynamics rules. Once again, the *hub*-based characteristic of the BA network resulted on massive attack against the disease. This type of attack can be identified by the great amount of eliminated disease in the reaction-diffusion constrained by the BA network (second snapshot in fig. 3-d) in contrast to the ER network (second snapshot in fig. 3-c). Because of the finite-size and sparse connectivity of both types of network, not enough neighbors nodes were requested, allowing leakage and subsequent relapsing of the disease. Due to the antidote liberation, the disease grew in the direction contrary to where the node were placed. Even the small disease

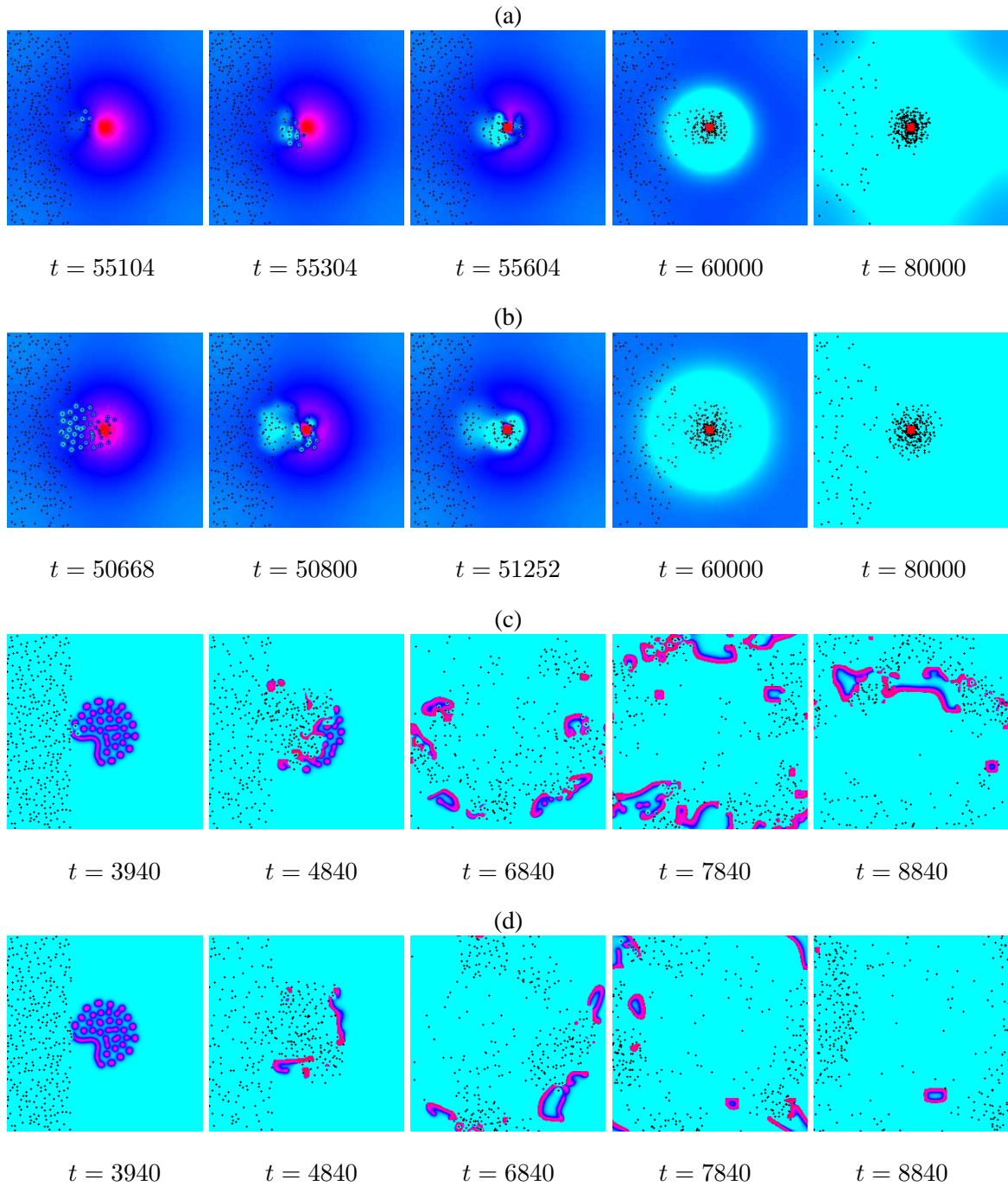


Figure 3: Snapshots of the pattern for the four cases: (a) Fick diffusion and ER network, (b) Fick diffusion and BA network, (c) Gray-Scott reaction-diffusion and ER network and (d) Gray-Scott reaction-diffusion and BA network. Red (on-line version) represents maximum disease intensity and cyan (on-line version) no disease. The node are represented by the black dots. Both networks have 300 nodes and $\langle k \rangle \approx 4$.

sources of the BA case produced much infection in the mesh after about 3000 time units from the first activation (third snapshot in fig. 3-d). However, the non-massive attacks of ER network nodes resulted on more isolated patterns and in faster increase of the disease quantity (third snapshot in fig. 3-c). After the interval of increase (fourth snapshot in fig. 3-c,d), the node retook control, eliminating many isolated patterns (fifth snapshot in fig. 3-c,d). While the node were eliminating many isolated patterns (fifth snapshot in fig. 3-c), a uniform spatial node distribution emerged in the mesh. Conversely, in the presence of few infected areas, the nodes joined efforts to eliminate them and concentrated themselves on the highest infected regions of the mesh (fifth snapshot in fig. 3-d). After the complete elimination of the disease, the node remained on their last respective positions. Observe that the original pattern was modified at the places where the antidote acted, specially near the activated node.

The ability of the defensive network to control and stop the disease was verified to be directly related to the number of node and to the connectivity of the network. We expected that with more node being activated, they would more readily gather control and completely eliminate the disease spreading. A larger and completely connected network would activate all the neighbors at once and hence fully populate the mesh. Consequently, the disease would fade down quickly until complete elimination. Such a network would imply high maintenance costs if adopted by natural (or artificial) systems. In fact, it is often mandatory to achieve maximum efficiency by using the minimum amount of energy. In practice, many of the networks which have been investigated in complex networks research are characterized by low connectivity among their node [1, 2, 3]. Therefore, it is interesting to investigate the efficiency of ER and BA networks with small number of node (relatively to the mesh size) and low connectivity, as in many natural and artificial real systems.

Figure 4-a compares the evolution of the amount of disease I for the Fick diffusion model using the *one-source* configuration. A total of 100 realizations was considered for each parameter configuration. The quantity I had a nearly constant growth rate up to a maximum, when the first node were activated. These node triggered a chain reaction, but on the average both networks had similar efficiency in controlling the diffusion in the beginning, *i.e.*, until about 60000 time units. The time spent to enclose the source was relatively short and, on average, no difference could be observed between both types of networks. The importance of *hub*-activation, implying liberation of more antidote, showed up after 60000 time units, when the diffusion constrained by the BA network clearly decreased faster than the diffusion observed for the ER network. By comparing

figures 4-a, 5-a and 6-a, it is clear, for both types of networks, that the diffusion dropped down and reached minimum levels faster when the number of defensive node and the connectivity of them were increased. However, BA network nodes continued to be more effective against the disease than the ER network nodes. Interestingly, the minimal level of diffusion was reached at nearly the same time in both types of networks in the first configuration ($N = 300$ and $\langle k \rangle \approx 4$) and about 20000 time units earlier in the BA case than in the ER case for the other two configurations ($N = 500$, $\langle k \rangle \approx 4$ and $\langle k \rangle \approx 6$), a consequence of the increased amount of antidote liberated in the first stages of the defense.

The non-uniform patterns generated by the Gray-Scott reaction-diffusion implied richer dynamics (fig. 3). Starting from the initial source, non-localized patterns emerged over time, creating fast moving spots and stripes, so that the nodes had to actively move through the regular network in order to eliminate the disease. The amount of disease increased in nearly quadratic fashion with time up to a maximum when the first node were activated. Depending on the connectivity of the defensive network, different evolutions were clearly obtained after the first activation. The reaction-diffusion constrained by networks with $\langle k \rangle \approx 4$ (see fig. 4-b and fig. 5-b), resulted on three stages: (i) a decrease down to a minimum level, (ii) a relapse up to a local maximum level and (iii) resumption of the decrease until the disease is eliminated. On the other side, the network with $\langle k \rangle \approx 6$ (see fig. 6-b) exhibited two stages: (i) fast and (ii) slow elimination of the disease. Observe that this phenomenon is not only due to the connectivity, but also depends on the number of nodes: a higher quantity of simultaneously activated nodes resulted in more antidote and, consequently, reduction of the disease (*i.e.* I).

The first stage of defense (between 4000 and 6000 time units), was a consequence of *hierarchical neighbors* activation [19]. Once the disease had considerably diffused along the space, every new request contributed to the distribution of more activated nodes radially to the boundary of the disease. Obviously, some nodes fell on positions without disease. It was also possible to have some nodes requested by their own requested neighbors. Because of the finite-size of the network, on the average the hierarchical number of neighbors had a peak n_{max} whose value depends on the number of nodes and on the connectivity of the network [20]. The presence of *hubs* implied that n_{max} is reached faster (in terms of *hierarchical levels*) in the BA than in the ER network. In other words, BA node activate more neighbors at once than the ER node in the first *hierarchical levels*. Therefore, in this stage the disease decreased faster in the BA than the ER case as shown in Figures 4-b, 5-b and 6-b. As expected, more node and higher connectivity implied on more

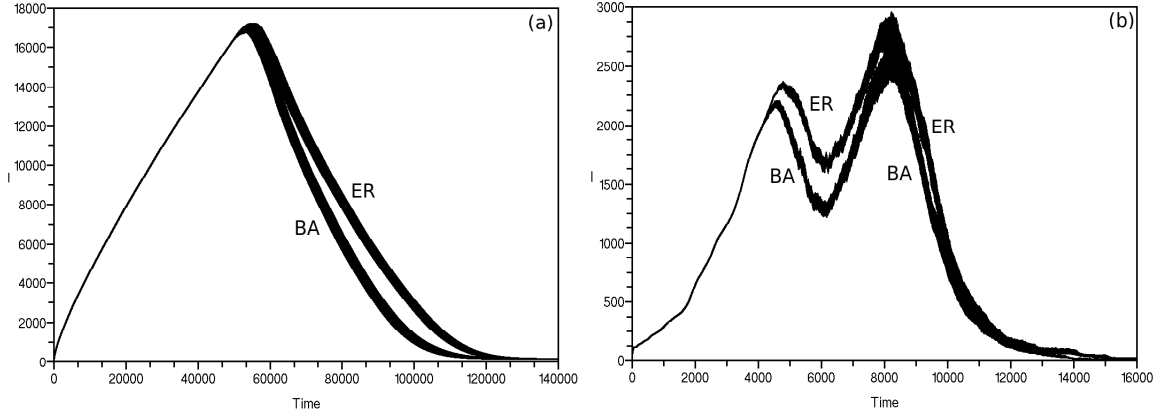


Figure 4: The amount of disease I in the mesh ($y - axis$) at time ($x - axis$). (a) Fick diffusion model and (b) Gray-Scott model. *One source*, $N = 300$ and $\langle k \rangle \approx 4$ configuration. The standard deviation is (a) one fifth and (b) one tenth of the real value.

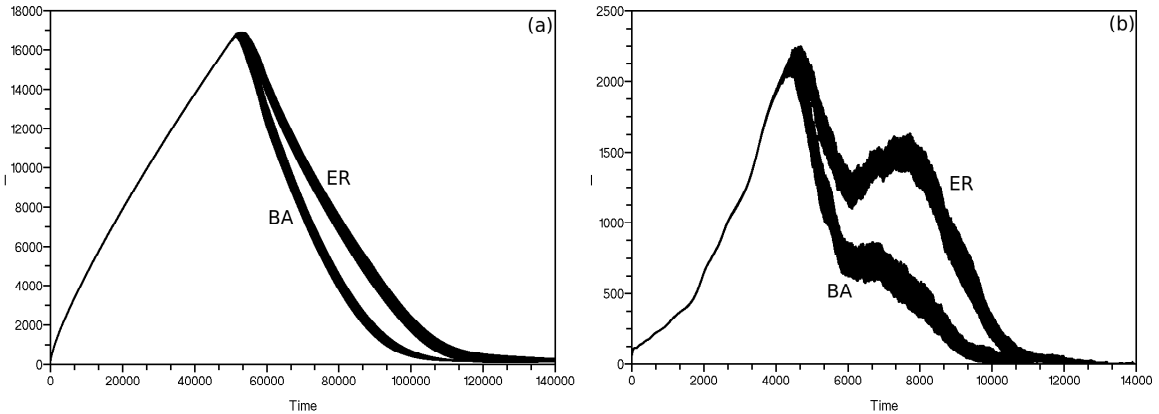


Figure 5: The amount of disease I in the mesh ($y - axis$) in terms of time ($x - axis$). (a) Fick diffusion model and (b) Gray-Scott model. *One source*, $N = 500$ and $\langle k \rangle \approx 4$ configuration. The standard deviations in this figure corresponds to one fifth of their real values.

effective decrease in the disease intensity.

The second stage of defense (between 6000 and about 8000 time units) was characterized by leakage of disease from the first massive attack (*i.e.*, chain reaction). The requested neighbors, in the first stage, were not enough to control the disease, *i.e.* although they broke the pattern, some isolated regions of disease concentration remained which resumed progression. ER networks tended to engage less nodes than BA networks, allowing the creation of a larger number of

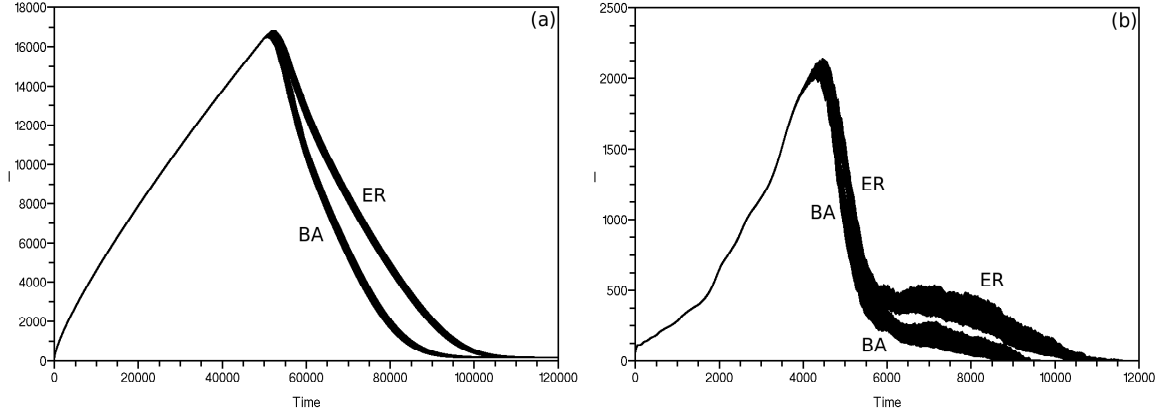


Figure 6: The amount of disease I in the mesh ($y - axis$) at time ($x - axis$). (a) Fick diffusion model and (b) Gray-Scott model. *One source*, $N = 500$ and $\langle k \rangle \approx 6$ configuration. The shown standard deviation is one fifth of its real value.

isolated patterns. The latter effect implied more competition for node, postponing the control of the disease. Figures 4-b and 5-b show that as the number of network nodes was increased, the relapse peak tended to diminish, *i.e.*, more node resulted in more effective control of the disease. The relapse peak depended considerably of the height of the disease intensity I at the turning point [21], *i.e.*. More distributed patterns implied in more intense relapse and increased difficult of respective control. The node had to swap their places constantly, following the requests which depended on the connectivity of the defensive network and not on the node distance in the regular network. Consequently, these movements of node resulted on vacancies in the regular network, which allowed the local development of disease. Observe that the effective elimination of disease by the latter network configuration, *i.e.*, $N = 500$ and $\langle k \rangle \approx 6$ (fig. 6-b), resulted in few remaining sources. Consequently, the defensive network was capable to control the disease and maintained a low level of disease prior to its complete elimination.

The third stage (between 8000 time units and the complete disease elimination, see fig. 4-b and fig. 5-b - absent in the third network configuration shown in Figure 6-b) was a consequence of the recovery of control by the activated nodes. Recall that due to the initial conditions, much antidote was liberated in the central area of the board in the first stage of defense. Naturally, the disease grew faster in the antidote-free regions, *e.g.* opposite to the central area. However, much antidote was also concentrated in other regions over time. This amount of already liberated antidote contributed to slowed down the growing rate of the disease. The fact that the node had

lesser disease to eliminate contributed to faster elimination of the infection. Interestingly, the long tail in the graphic in Figures 6-b, 7-b and 8-b was a result of some small steady sources enclosed by the antidote, these sources was not eliminated but could not grew too. Under this situation, an equilibrium was ultimately established where any growth of the disease was promptly eliminated by antidote being liberated by the surrounding node. The latter behavior was also identified before the disease elimination in the third network configuration (fig. 6-b).

The competition for node played a fundamental role in the proposed dynamics since help requests implied on depletion of node which were previously activated. If a neighbor j was helping a node and another node requested help from j , that node changes its position with 50 per cent of probability. Recall that node request as a consequence of high activity in the regular network has priority over solicitations by neighboring nodes. As a consequence, only regular network activated nodes did not change their positions while at this state. Given the degree distribution of ER and BA networks, we expected improvement in the ability of disease control to be observed for the ER network. The more uniform distribution of degrees in the former type of network resulted in a better management of the distribution of node among many disease focuses. Conversely, the request of many node by *hubs* tended to unbalance the number of node at each infected area.

We also investigated the evolution of the disease when two sources were established as initial conditions. Once again, a total of 100 realizations was considered for each parameter configuration. The resulting shape of the curves was similar to that observed for the *one-source* configuration. Naturally, the Fick diffusion with two symmetrically displaced sources resulted in faster increase in the total amount of disease, so that the threshold was quickly overcome (about 20000 time units before the *one-source* case - fig. 7-a, fig. 8-a and fig. 9-a). The main strategy against the Fick diffusion is to enclose the sources, which was obtained as soon as the chain effect was triggered. Afterwards, the node only had to keep generating antidote in order to completely eliminate the already spread disease. A disease decrease rate similar to the *one-source* configuration was also expected. Once many node were still in their original positions, there were many susceptible nodes to be shared between the sources. Another interesting effect occurred when one of the sources engaged all of the available node. The control of the second source turned out to be indirect, *i.e.* due to the antidote generated by the node activated by the first source. The latter effect slowed down the elimination of the disease and increased its minimal level along the last steps, since the antidote could not reach the source as effectively as could be achieved by node displacement. This effect implied higher standard deviation of the disease intensity I , specially at

its minimal levels.

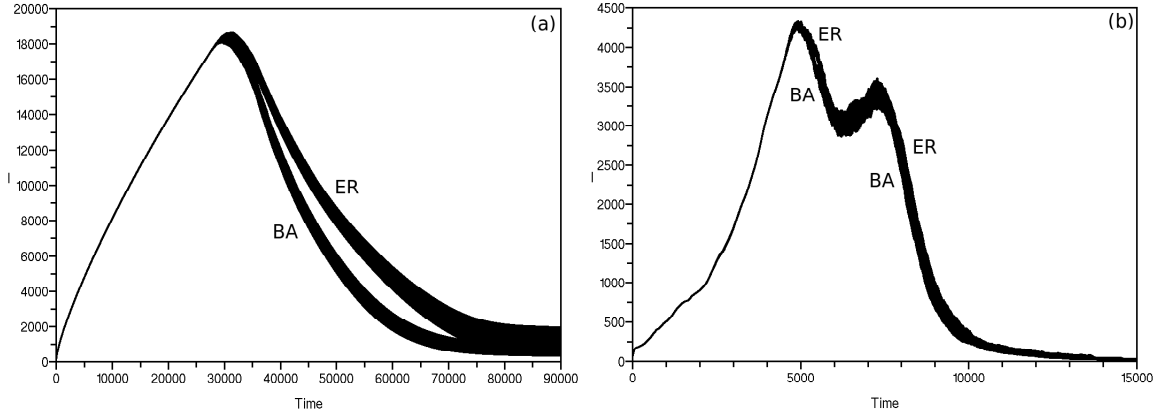


Figure 7: The amount of disease I in the mesh ($y - axis$) along time ($x - axis$). (a) Fick diffusion model and (b) Gray-Scott model. *Two sources*, $N = 300$ and $\langle k \rangle \approx 4$ configuration. The standard deviation are shown at one fifth (a) and one tenth (b) of their real values.

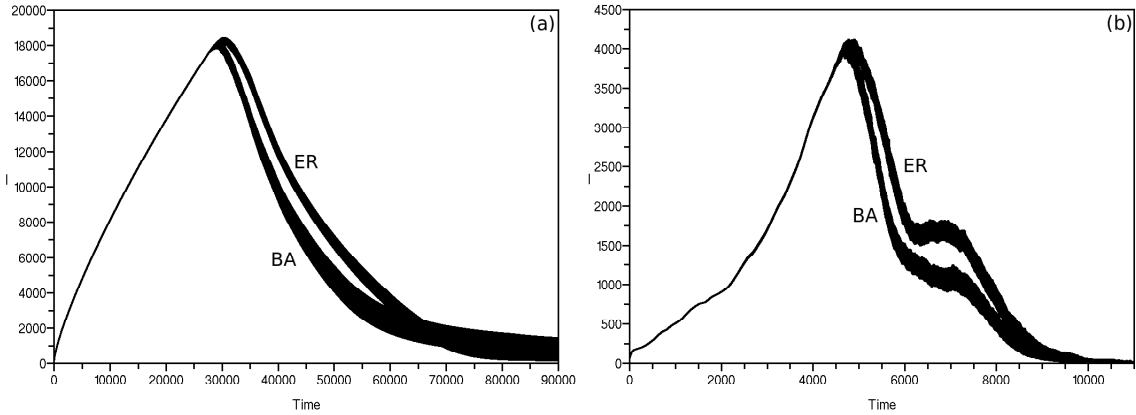


Figure 8: The amount of disease I in the mesh ($y - axis$) along time ($x - axis$). (a) Fick diffusion model and (b) Gray-Scott model. *Two sources*, $N = 500$ and $\langle k \rangle \approx 4$ configuration. The standard deviation is shown at one fifth of its real value.

The configuration with higher number of nodes and connectivity (fig. 8-a and fig. 9-a) resulted on decrease of the efficiency in the BA network in the last stage of the defense dynamics. The uniform distribution of ER connections resulted on average in a higher efficiency in the enclosement of both sources. Over time, ER better managed the swapping of node between both sources. On the other hand, *hubs* requests ER resulted in a higher concentration of node around one of the sources

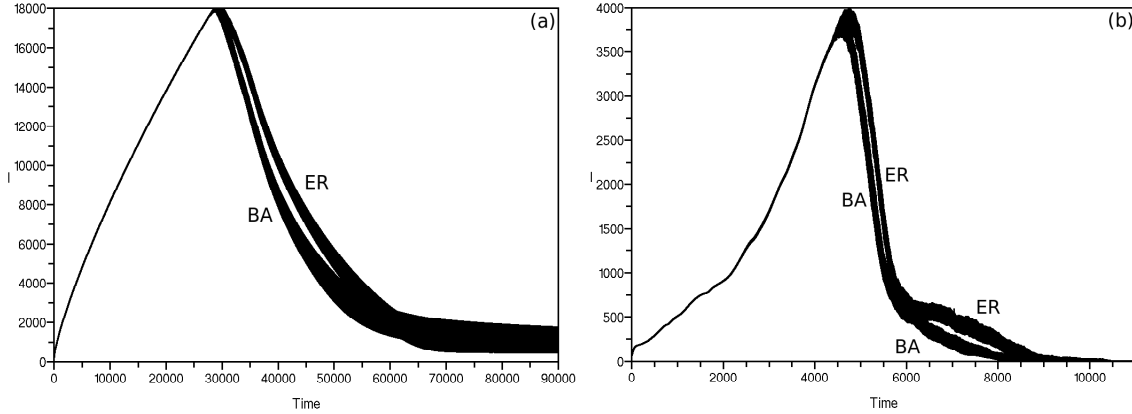


Figure 9: The amount of disease I in the mesh ($y - axis$) along time ($x - axis$). (a) Fick diffusion model and (b) Gray-Scott model. *Two sources*, $N = 500$ and $\langle k \rangle \approx 6$ configuration. The standard deviation is shown at one fifth of its real value.

(*e.g.*, source 1). Consequently, the node were hardly activated due to the disease generated by the other source (*e.g.*, source 2). The latter effect diminished the elimination rate of the disease because one of the sources (*e.g.*, source 2) turned out to be indirectly controlled, *i.e.*, through the antidote generated only by the node which were activated by the first source (*e.g.*, source 1).

The initial effect of the two sources in the Gray-Scott model was the creation of two large infected areas on both sides of the wall of nodes. Each of them had approximately the same size as the area generated by the *one-source* configuration. The total amount of disease before the first activation was nearly twice as much in the *two-sources* configuration than observed for the *one-source* case. Consequently, when the spots and stripes reached the node, they initially had a larger amount of disease to eliminate. The same three stages were identified (fig. 7-b) as in the *one-source* case. However, the uniform distribution of neighbors in the ER network favored a better distribution of the node among the many infected areas. This effect contributed to improve the defense ability of the network and enhanced its efficiency. On the other hand, *hubs* made massive attacks against large infected areas. However, they requested many node which were defending other areas. The same effect contributed to the appearance of the second peak in figure 4-b. The increase of network node (fig. 7-b) resulted in better control of the disease constrained by the ER network. In fact, the second peak (relapse) was absent in this case. Finally, the increase in the connectivity of the network, resulted in even faster elimination of the disease. In the average, each request engaged more node, which contributed to the steady reduction of the amount of disease.

V. CONCLUSIONS

Many natural phenomena involve interactions between two or more independent *sub-systems* with specific properties (*e.g.*, firemen combating forest fire, infection spreading into a healthy tissue while interacting with defensive cells, cleaners controlling oil spilling, pest control, *etc.*). The structure of each *sub-system* can be modeled in terms of a network while the dynamics is represented by processes occurring in each network (*e.g.*, the movement of agents or pattern formation). An interaction rule couple both *sub-systems* in such a way that the evolution of one *sub-system* depends on the other one and *vice-versa*. Since the connections are responsible for the way the defensive agents communicate, they play a fundamental role in the behavior of such complex systems, *i.e.* they control the dynamical evolution of the agents (*i.e.*, node) which in turn, constrains the evolution of the dynamical pattern. For example, the specific way in which groups of firemen are organized determines whether they will control or not the fire spreading. Similarly, the signal connectivity of anti-bodies (*i.e.*, complex network) is crucial to efficiently activate them to stop an infection diffusion through a healthy tissue.

To investigate such phenomena, we proposed a dynamical hybrid system composed of a regular and a complex network. The complex network represented connected defensive agents (*i.e.*, node) self-organizing to eliminate patterns evolving in the regular network which in turn, represented the unwanted process. According to the local pattern intensity, the node were activated to liberate an opposite diffusion aiming to eliminate the pattern. Two pattern growth models were considered: Fick diffusion and Gray-Scott reaction-diffusion. The defensive agents were connected following Erdős-Rényi and Barabási-Albert models. Two types of initial conditions were investigated: *one-source* and *two-sources*. The role of the network structure was investigated by using three network configurations: (i) $N = 300$ and $\langle k \rangle \approx 4$ (ii) $N = 500$ and $\langle k \rangle \approx 4$ (iii) $N = 500$ and $\langle k \rangle \approx 6$.

The main results included the better performance obtained by the BA comparatively to the ER network to any chosen configuration. The *hub*-based characteristic of the BA network provided massive attacks against the disease. Heavy defense was crucial in the beginning in order to fast accelerate the ratio of decrease of the amount of disease in the regular network. These massive attacks avoided much leakage and emergence of isolated patterns which were present at higher rates in the ER case. Isolated patterns were responsible for the relapse of the disease. The increase in the number of network nodes and in their connectivity contributed significantly to faster eliminate the disease. These results have shown the importance of *hubs* in defensive networks. *Hubs* contribute

to diminish the *average path length* in the network. Consequently, on average the hierarchical level with maximum number of nodes can be reached earlier in the BA than in the ER network. As a result, a more effective defense can be evaluated when the disease is concentrated in a large area. On the other side, despite of the better efficiency of the BA network, the uniform distribution of nodes in the ER network contributed to efficient defense strategies when many isolated patterns emerged on different places in the regular network.

Future developments include: (i) investigation of optimal network structure to efficiently eliminate the pattern, (ii) analysis of how the system properties scale with its size, (iii) study of the pattern evolution under network perturbations (*e.g.*, node attack or edge rewiring), and (iv) improvement of the model by inclusion of other communication protocols taking place in the defensive network, such as broadcasting.

Acknowledgments

LECR is grateful to CNPq for financial support. LFC is grateful to CNPq (308231/03-1) and FAPESP (05/00587-5) for financial support.

-
- [1] M. E. J. Newman, *SIAM Reviews* **45**, 167 (2003).
 - [2] S. N. Dorogovtsev and J. F. F. Mendes, *Advances in Physics* **51**, 1079 (2002).
 - [3] R. Albert and A.-L. Barabási, *Reviews of Modern Physics* **74**, 47 (2002).
 - [4] S. N. Dorogovtsev and J. F. F. Mendes, *Evolution of Networks, From Biological Nets to Internet and WWW* (Oxford University Press, Oxford, 2003).
 - [5] L. d. F. Costa, F. A. Rodrigues, G. Travieso, and P. R. Villas Boas, *Characterization of complex networks: A survey of measurements* (2005), e-print arXiv:cond-mat/0505185.
 - [6] A. E. Motter, *Physical Review Letters* **93**, 098701 (2004).
 - [7] N. Madar, T. Kalisky, R. Cohen, D. ben Avraham, and S. Havlin, *European Physical Journal B* **38**, 269 (2004).
 - [8] L. K. Gallos and P. Argyrakis, *Physical Review E* **72**, 017101 (2005).
 - [9] J. D. Noh and H. Rieger, *Physical Review Letters* **92**, 118701 (2004).
 - [10] P. Erdős and A. Rényi, *Publicationes Mathematicae* **6**, 290 (1959).

- [11] A.-L. Barabási and R. Albert, *Science* **286**, 509 (1999).
- [12] J. Crank, *The Mathematics of Diffusion* (Oxford University Press, Oxford, 1980).
- [13] J. E. Pearson, *Science* **261**, 189 (1993).
- [14] H. S. Carslaw and J. C. Jaeger, *Conduction of Heat in Solids* (Oxford University Press, Oxford, 1986).
- [15] L. Kadanoff, *Statistical Physics: Statics, Dynamics, and Renormalization* (World Scientific, Singapore, 2000).
- [16] P. Wilmott, S. Howison, and J. Dewynne, *The Mathematics of Financial Derivatives: A Student Introduction* (Cambridge University Press, Cambridge, 1995).
- [17] P. Okubo and S. A. Levin, *Diffusion and Ecological Problems: Mathematical Models* (Springer Verlag, Berlin, 1980).
- [18] P. Grindrod, *The Theory and Applications of Reaction-Diffusion Equations: Patterns and Waves* (Oxford University Press, Oxford, 1996).
- [19] L. d. F. Costa and L. E. C. da Rocha, *European Physical Journal B* **50**, 237 (2006).
- [20] L. d. F. Costa and F. Nascimento, *Hierarchical characterization of complex networks* (2005), e-print arXiv:cond-mat/0412761, to appear in *Journal of Statistical Physics*.
- [21] The turning point corresponds to the abscissae of the relative minimum of the disease intensity I , which tended to occur nearly after 6000 steps.